Using X-ray Flux Time Series for Solar Explosion Forecasting

Ismael Caldana, Ana Estela Antunes da Silva, Guilherme Palermo Coelho, and André Leon S. Gradvohl
School of Technology (FT), University of Campinas (UNICAMP)
Limeira-SP, Brazil
E-mails:ismaelcaldana@outlook.com, {aeasilva, guilherme, gradvohl}@ft.unicamp.br

***Abstract*—Among the natural phenomena that happen in the Sun, one that has direct impact on Earth are the solar explosions. These explosions emit an X-ray flux that can be detected and used as an indicative of new explosions. In this work, we evaluated whether X-ray flux time series are suitable as the base dataset for solar flare forecasting. To do so, we applied a multilayer perceptron (MLP) neural network and performed a series of experiments to identify its best parameters and its performance for different forecast horizons. The experiments indicated that X-ray flux time series can be used to forecast solar flares and that MLPs are capable of properly forecasting future values of the time series, even though the average errors increase with wider forecast horizons. Besides, we also observed that qualitative analyses are essential for solar explosion forecasts, and should also be made together with traditional quantitative analyses of the results.**

1. Introduction

Solar flares are explosions on the surface of the Sun caused by sudden changes in the magnetic field of its surface. An explosion occurs when magnetic fields of different polarities around the Sun approach and create magnetic arcs [1], [2].

Although the solar flares are not the riskiest solar events, they are often related to the emission of energetic particles and the ionization of Earth's high atmosphere. Besides, about 70% of solar flares precede the noxious and less frequent coronal mass ejections [3]. Their consequences can affect the satellite orbit, cause interruptions in the distribution of energy in the electrical grid, disturbances in the radio waves and in navigation systems, among others [4], [5]. Thus, it is important to predict the occurrence and intensity of solar explosions.

The X-ray flux is usually part of the set of input parameters of machine learning algorithms for classification and prediction of solar explosions [6]. The flux, measured in Watts per square meter (W/m^2), is used on a logarithmic scale that divides the eruptions into the categories: A, B, C, M and X (from lowest to highest intensity). These categories, in turn, have a more precise division according to a multiplication factor ranging from 1 to 9 (except for class X that has no upper limit) [2]. Space observation instruments, such as the GOES-15 satellite [7], record solar activity parameters, collecting minute-by-minute data and providing the records neatly, forming time series. These series can allow the estimation of future values of these same series in a short or long term [8].

In order to obtain predictions for the occurrence of solar explosions from these data, it is necessary to use a computational model that works with data series and can identify patterns, such as the continuous growth of X-ray flux in a range, which may characterize an explosion. A possible mechanism to perform this task are artificial neural networks, which are capable of learning from this data and of identifying patterns and interpreting new samples through what has been learned [9].

The main aim of this study was to establish the possibility of using X-ray flux as a predictive parameter of solar flares. A Multilayer Perceptron (MLP) neural network was applied to the X-ray flux time series obtained from the GOES-15 satellite from January 1, 2014 to December 31, 2014, as this range is situated in the solar maximum of cycle number 24. Several experiments were conducted and the results showed that such prediction is possible if short forecasting horizons are considered.

2. Related works

In the literature, there are several approaches for predicting solar activity and solar explosions. Most of these approaches differ from the proposal of this work, which hinders a direct and quantitative comparison. Thus, this section cites the main works in the field of application of machine learning to the problem of solar explosions that involve the following themes: prediction and classification of solar explosions, especially those that use X-ray fluxes as an input parameter and employ artificial neural networks.

In [10], a hybrid model that combines image processing of the solar corona for identification, grouping, and classification of sunspots using machine learning algorithms was proposed, with the focus on the analysis of an extensive record of sunspot and solar explosions data. The proposed system is intended to provide predictions of solar explosions in the short term. A Multi-Layer Perceptron neural network (MLP) is also used to process historical data about solar activity. However, the neural network output is associated with the probability of occurrence of high-intensity solar

explosions in a given period, rather than the predictions of values of a time series.

Ahmed et al. [11] proposed a model that associates feature extraction, image processing and machine learning algorithms. To this end, they applied image processing to solar magnetograms in order to extract relevant characteristics. A Cascade Correlation Neural Network (CCNN) processes historical datasets of the occurrence of solar explosions, and finally applies feature extraction algorithms to detect and characterize different magnetic properties. Such feature extraction is made according to the potential of prediction and the relevance of the features in relation to the occurrence of solar explosions.

Bobra & Couvidat [6] proposed the use of Support Vector Machines (SVMs), applied to historical data of the solar magnetic field, to determine which active regions of the solar corona would give rise to solar explosions. In this case, X-ray flux data were also taken into account to classify the solar explosions in relation to their intensity, categorizing the flares into M and X classes. To that end, the SVMs were trained with a set of positive or negative instances to classify the active regions by the occurrence or not of solar explosions.

The dataset adopted in [6] was previously submitted to feature extraction and selection procedures, in order to filter the most relevant attributes for classification purposes. Also to improve the predictive capacity of the model, Bobra & Couvidat [6] adopted a procedure to balance the proportion of positive and negative samples, which was achieved by assigning different cost parameters for each class. This model led to results with relatively high precision when compared to the original works from which it was derived and indicated, as a future research, the attempt to classify not only the occurrence or not of the solar explosions, but also its intensity (for classes M or X) in positive examples.

Calvo et al. [12] reinforced the idea that artificial neural networks are a suitable way to analyze time series since they are capable of generalizing the dynamics of solar activity and generating good long-term predictions. For this, the authors used datasets related to the number of Wolf, which indicates the number of visible sunspots and is one widely adopted indicator of the intensity of solar activity.

Orfila et al. [13] described the use of a variant of a genetic algorithm for predicting the number of sunspots in the long term, with 1, 3 or 5 years in advance. The results presented in [13] indicate that the genetic algorithm is particularly appropriate for time series based on nonlinear models, such as the solar activity cycle, and can be useful to similar tasks, such as the prediction of solar activity.

Differently from the works previously mentioned, the present work isolates the X-ray flux as the only attribute considered in the prediction of solar activities and tries to identify suitable MLP configurations to expand the forecasting horizon. In the next section, the methodology used in this work is explained.

3. Methodology

In order to verify whether the X-ray flux time series can be used as the main data source for solar flare forecasting, minute-by-minute historical readings obtained by the GOES-15 satellite from January 1, 2014 to December 31, 2014 were used here. These data, which are organized and constantly published on-line by the Space Weather Prediction Center – SWPC [7], was downloaded, reorganized and stored locally, so it could be preprocessed and used to train the Multilayer Perceptrons configured to forecast future values of the X-ray flux.

Two preprocessing steps had to be made before the experiments: (*i*) the imputation of missing values in the dataset, with the average between the two closest valid values (one immediately before and the other immediately after the missing value); and (*ii*) the normalization of the time series values between 0 and 1, so that they become suitable to be used with the MLPs considered here (such MLPs adopt logistic activation functions in the hidden and output layers).

Three sets of experiments were performed here and the results were evaluated both qualitative and quantitatively. The quantitative analysis was made with the average and standard deviation of the mean-squared prediction errors, as detailed in Section 3.4. The qualitative analysis, on the other hand, required visual inspections of the graphical representations of both the original and forecast X-ray flux time series. Such visual inspection was important to verify whether there are no delays between the peaks of both series, which would directly result in a delay of the solar flare forecast.

The topologies of the MLPs were defined based on the smaller MSE obtained after numerous tests with different amounts of layers and neurons per layer. In the following subsections, the three sets of experiments performed here will be described, together with the quantitative metrics adopted to evaluate the results.

3.1. One MLP for multiple forecast horizons

The first set of experiments was aimed at identifying the MLP training algorithm that leads to the smallest X-ray flux forecast errors for different forecast horizons. Therefore, five algorithms were evaluated here: *Quick Propagation*, *Resilient Propagation*, *Manhattan Propagation*, *Backpropagation* and *Scaled Conjugate Gradient* [14], [15].

As previously mentioned, the X-ray flux time series considered here contains values evaluated minute by minute, which is essential for solar flare forecasting: when solar flares occur, they provoke perturbations in the X-ray fluxes that lasts a few minutes. Therefore, three different forecast horizons were considered here: (*i*) one minute ahead forecasts, which is not very useful in practice but allows the verification of the proposed methodology; (*ii*) five minute ahead forecasts; and (*iii*) ten minute ahead forecasts. To do so, one MLP with multiple outputs, one for each forecast

horizon, was adopted. The detailed topology of such MLPs is:

- **Input Data:** 5 values, which correspond to 5 consecutive historical values of the time series immediately before the first value to be forecast by the MLP;
- **First Hidden Layer:** 5 neurons with logistic activation functions;
- **Second Hidden Layer:** 10 neurons with logistic activation functions;
- **Output Layer:** 10 neurons (one for each forecast horizon) with logistic activation functions.

3.2. Different MLPs for different forecast horizons

After the identification of the best training algorithm in the first set of experiments, a second topology of MLPs was also evaluated here. In this second topology, one MLP for each forecast horizon (thus with a single output) was trained. The rationale was to verify whether MLPs specialized for each forecast horizon would obtain smaller forecast errors when compared with those of a single MLP responsible for dealing with several different horizons.

The summary of each MLP topology in this second set of experiments is:

- **Input Data:** 5 values, which correspond to 5 consecutive historical values of the time series immediately before the first value to be forecast by the MLP;
- **First Hidden Layer:** 5 neurons with logistic activation functions;
- **Second Hidden Layer:** 10 neurons with logistic activation functions;
- **Output Layer:** 1 neuron with logistic activation function.

3.3. Balancing the training samples

Finally, the third set of experiments performed here adopted the same MLP topology presented in Section 3.2, but now trained with a *balanced* dataset.

Considering that the M and X classes of solar flares (which result in X-ray flux peaks in the $[10^{-5}; 10^{-4}]$ interval and above 10^{-4} threshold, respectively) do not happen very often, the X-ray flux time series does not contain many data samples that represent these two phenomena. Therefore, the original dataset is imbalanced in terms of the numbers of instances of each possible class. This can be an issue, as the MLPs trained with such imbalanced dataset may not be able to properly forecast solar flares of classes M and X, which are the most intense ones and often result in severe consequences on Earth. Table 1 shows the number of instances and the percentages of each class of flares in the dataset before and after balancing.

Therefore, after the time series was converted into a set of input-output samples to be used in the training phase of the MLPs, the expected output value of each training sample was analyzed and an undersampling procedure was adopted [16]. Such procedure randomly eliminates samples associated with major classes. Hence the final training dataset ends up with similar numbers of training samples associated with each solar flare class. The rationale here was to guarantee that the MLPs would be trained with a set of data samples that represent the highest peaks of X-ray flux (which are associated with M and X class flares).

TABLE 1. PERCENTAGE OF SAMPLES FOR EACH CLASS OF FLARES.

	Before Balancing		After Balancing	
Class	# of instances	Percentage	# of instances	Percentage
A	169	0.03%	1	0.03%
B	297841	56.7%	264	20.59%
C	220917	42.1%	341	23.75%
M	6296	1.19%	338	27.29%
X	371	0.07%	371	28.34%

3.4. Results Evaluation

To quantitatively assess the results obtained here, each experiment was repeated 5 times and the average and standard deviations of the forecasting errors were evaluated. For each repetition of each experiment, the Mean Squared Error (MSE) of the forecasts, given in Eq. 1, was calculated.

$$MSE = \frac{\sum_{i=1}^{N}(idealValue - obtainedValue)^2}{N} \quad (1)$$

where $idealValue$ is the expected output of the MLP for a given input sample, $obtainedValue$ is the output of the MLP for such sample and N is the number of samples in the dataset.

Given that each experiment was repeated $M = 5$ times, the Average Mean Squared Error of the forecasts ($\overline{MSE}$), given in Eq. 2, was adopted to evaluate the general performance of each MLP.

$$\overline{MSE} = \frac{\sum_{i=1}^{M}(MSE)}{M} \quad (2)$$

Finally, to evaluate the variation of the obtained results during the $M = 5$ repetitions of the experiments, the standard deviation of the MSE, given in Eq. 3, was also considered here.

$$\sigma = \frac{\sqrt{\sum_{i=1}^{M}(MSE_i - \overline{MSE})^2}}{M-1} \quad (3)$$

4. Experimental Results

The experiments carried out here followed the methodology presented in Section 3 and had two main goals: (*i*) verify whether X-ray flux time series could be used as the main data source for solar flare forecasting; and (*ii*) identify a MLP configuration suitable to perform forecasts with horizons larger than $T + 1$ (one minute ahead).

To do so, different MLP configurations were evaluated and three forecasting horizons were considered: one minute ahead ($T+1$), to validate the methodology, five minutes ahead ($T+5$) and ten minutes ahead ($T+10$). The experiments will be presented here in the same order adopted in Section 3.

4.1. Comparison between training algorithms

In this first experiment, the average performance of five well-known MLP training algorithms was analyzed. Five training sessions (repetitions) were performed with each algorithm, being each one limited to ten thousand iterations (epochs). For this experiment, the MLP topology mentioned in Section 3.1 was used: each network had 10 outputs, being the first one associated with the $T+1$ forecast, the second one with the $T+2$ forecast and so on. The summary of the obtained results for $T+1$, $T+5$ and $T+10$ are shown in Table 2.

Although $T+1$ (one minute ahead) forecasts are not too relevant in practice, they were kept in the analyses performed here to validate the algorithms, since they should present less predictive complexity when compared to moments more distant in time. Therefore, as shown in Table 2, all training algorithms presented low $\overline{MSE}$ for $T+1$, with Quick Propagation leading to the best results.

It can also be observed from Table 2 that, from the different algorithms considered here, Quick Propagation presented the lowest values of $\overline{MSE}$ for all forecasting horizons. Therefore, it was chosen as the standard training algorithm for the following experiments.

4.2. One MLP for each forecast horizon

In order to verify whether the $\overline{MSE}$ can be improved, a new network topology was used in this second part of the experiments. Now, there is a single output in each MLP, that is supposed to forecast the time series for one horizon only. For example, considering that $T+5$ is chosen as the forecasting horizon, this output value will correspond to the forecast value 5 minutes ahead from the current instant. For each forecasting horizon, five training sessions (repetitions) with a limit of ten thousand iterations (epochs) were carried out. The training algorithm used was the Quick Propagation, according to the results reported in Section 3.1.

Table 3 presents the results obtained with this new topology (together with the best results reported in Table 2, for comparison). It is possible to notice that there was an improvement in terms of the $\overline{MSE}$ when the new topology with a single output was adopted.

However, with this new topology, a forecasting delay was observed. To illustrate, figures 1 and 2 show two cuts of the time series for $T+5$ and $T+10$ forecast horizons, respectively. In Figure 1, it is possible to notice that, although the forecast series is very close to the original one, a small delay in time can be observed. Such delay is significantly higher when $T+10$ is considered, as can be seen in Figure 2.

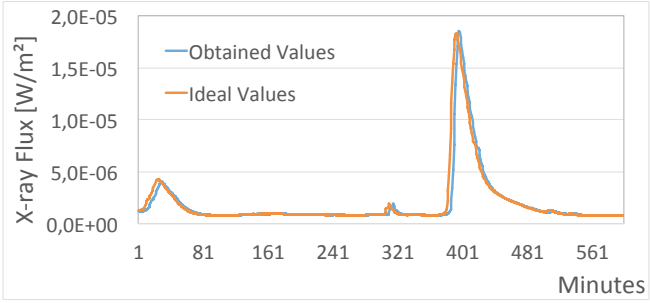

Figure 1. Cut of the original (in orange) and forecast (in blue) series, for a $T+5$ forecast horizon, obtained by an MLP with a single output.

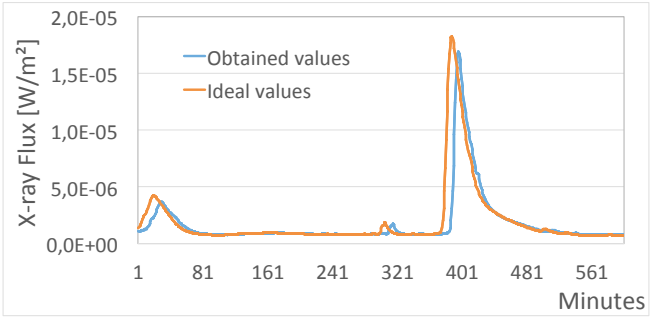

Figure 2. Cut of the original (in orange) and forecast (in blue) series, for a $T+10$ forecast horizon, obtained by an MLP with a single output.

These delays indicate that the MLPs may be actually "replicating" its inputs in the output and not forecasting future values of the time series. This can be a serious issue for solar flare forecasting, as it is vital to properly forecast the peaks of the X-ray time series. And this is not

TABLE 2. AVERAGE ± STD. DEVIATION OF THE MEAN-SQUARED ERROR (EQS. 2 AND 3) OBTAINED BY MLPS CONFIGURED WITH 10 OUTPUTS AND TRAINED WITH FIVE DIFFERENT ALGORITHMS. THE BEST RESULTS ARE HIGHLIGHTED IN BOLD.

Algorithm	$T+1$	$T+5$	$T+10$
Quick Propagation	$\mathbf{1.86 \times 10^{-13} \pm 5.06 \times 10^{-14}}$	$\mathbf{2.51 \times 10^{-12} \pm 1.63 \times 10^{-13}}$	$\mathbf{8.07 \times 10^{-12} \pm 1.65 \times 10^{-13}}$
Resilient Propagation	$7.81 \times 10^{-13} \pm 4.50 \times 10^{-13}$	$3.59 \times 10^{-12} \pm 2.28 \times 10^{-12}$	$8.13 \times 10^{-12} \pm 5.71 \times 10^{-13}$
Manhattan Propagation	$8.65 \times 10^{-12} \pm 4.16 \times 10^{-12}$	$1.42 \times 10^{-11} \pm 7.58 \times 10^{-12}$	$1.86 \times 10^{-11} \pm 2.58 \times 10^{-12}$
Back Propagation	$1.09 \times 10^{-11} \pm 4.98 \times 10^{-12}$	$1.24 \times 10^{-11} \pm 3.38 \times 10^{-12}$	$1.99 \times 10^{-11} \pm 6.85 \times 10^{-12}$
Scaled Conjugate Gradient	$1.85 \times 10^{-11} \pm 1.30 \times 10^{-11}$	$1.96 \times 10^{-11} \pm 1.18 \times 10^{-11}$	$2.19 \times 10^{-11} \pm 8.94 \times 10^{-12}$

TABLE 3. AVERAGE ± STD. DEVIATION OF THE MEAN-SQUARED ERROR (EQS. 2 AND 3) OBTAINED BY MLPS CONFIGURED WITH ONE OUTPUT (ONE MLP FOR EACH FORECAST HORIZON). THE BEST RESULTS ARE HIGHLIGHTED IN BOLD.

Neural Network Version	$T+1$	$T+5$	$T+10$
Ten Outputs Topology	$1.86 \times 10^{-13} \pm 5.06 \times 10^{-14}$	$2.51 \times 10^{-12} \pm 1.63 \times 10^{-13}$	$8.07 \times 10^{-12} \pm 1.65 \times 10^{-13}$
Single Output Topology	$\mathbf{1.25 \times 10^{-13} \pm 5.85 \times 10^{-14}}$	$\mathbf{2.13 \times 10^{-12} \pm 1.28 \times 10^{-13}}$	$\mathbf{7.44 \times 10^{-12} \pm 1.74 \times 10^{-13}}$

TABLE 4. AVERAGE ± STD. DEVIATION OF THE MEAN-SQUARED ERROR (EQS. 2 AND 3) OBTAINED BY MLPS CONFIGURED WITH ONE OUTPUT AND TRAINED WITH THE BALANCED DATASET. THE BEST RESULTS ARE HIGHLIGHTED IN BOLD.

Dataset	$T+1$	$T+5$	$T+10$
Inbalanced Dataset	$1.25 \times 10^{-13} \pm 5.85 \times 10^{-14}$	$\mathbf{2.13 \times 10^{-12} \pm 1.28 \times 10^{-13}}$	$\mathbf{7.44 \times 10^{-12} \pm 1.74 \times 10^{-13}}$
Balanced Dataset	$\mathbf{7.49 \times 10^{-14} \pm 1.84 \times 10^{-14}}$	$5.21 \times 10^{-12} \pm 4.10 \times 10^{-13}$	$3.04 \times 10^{-11} \pm 1.77 \times 10^{-12}$

happening here, although the $\overline{MSE}$s are low. Therefore, in order to improve the MLP learning process, a modification to the training dataset was proposed and the third set of experiments were performed.

4.3. MLPs trained with a balanced dataset

As mentioned in Section 3.3, explosions of classes M and X are rare events. Thus, the number of samples of X-ray flux values associated with these classes, in the dataset considered here, was extremely lower than the number of samples associated with classes B and C, for example (see Table 1).

In order to improve the MLP learning process, the data used in the experiments were submitted to a balancing process. This process, which is basically an undersampling approach [16], analyzes the desired output of the MLP training samples[1] and, according to their values, identifies whether each sample can be associated or not with a flare. If it indicates a flare, the class to which it belongs is also identified. After that, some of the samples that belong to the major classes in the dataset (those with the highest number of samples) are randomly eliminated, so that the samples of classes B, C, M and X were kept in similar percentage.

At the end of the balancing process, MLPs with the same topology reported in Section 3.2 were trained. Table 4 shows the average and the standard deviation of the results obtained after five repetitions for each forecast horizon. Each training procedure was limited to one thousand iterations.

From the results reported in Table 4, it is possible to notice that there was an improvement in terms of the $\overline{MSE}$ only for $T+1$, compared to the results reported in Table 3. However, as can be seen from figures 3 and 4 (for $T+5$ and $T+10$), the temporal delay between the original and forecast time series was eliminated. Figures 3 and 4 also show that these new results present an offset in the X-ray flux values, which led to the higher values of $\overline{MSE}$ observed in Table 4.

When the focus of the forecast is to identify future solar explosions, it is mandatory that the peaks of the X-ray flux series are synchronized with those observed in the original data. Otherwise, dangerous explosions can be missed and the overall purpose of the forecasting system is lost.

Therefore, from the results observed here, it is possible to conclude that a qualitative analysis of the forecast results (the graphical observation of the series) is as important as a quantitative analysis ($\overline{MSE}$ values) in the context of solar flare forecasting. Otherwise, the user may be led to false conclusions.

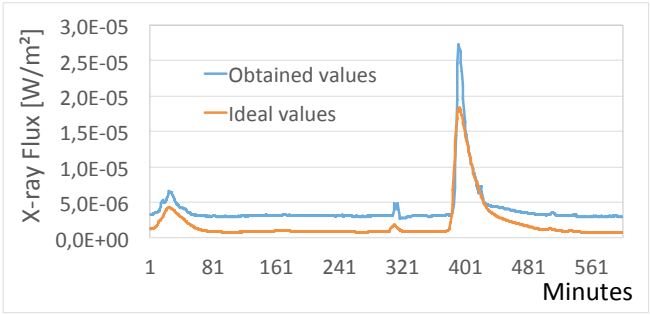

Figure 3. Cut of the original (in orange) and forecast (in blue) series, for a $T+5$ forecast horizon, obtained by an MLP with a single output and trained with a balanced dataset.

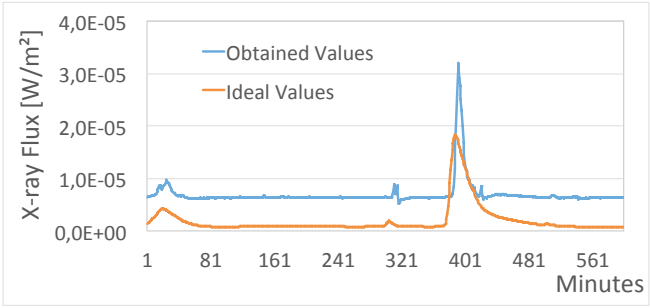

Figure 4. Cut of the original (in orange) and forecast (in blue) series, for a $T+10$ forecast horizon, obtained by an MLP with a single output and trained with a balanced dataset.

1. The training samples are obtained after the time series is preprocessed and corresponds to a modified dataset in which each sample is composed of the inputs for the MLP and the expected output.

5. Conclusion

In this work, we have evaluated whether X-ray flux time series is suitable to be used to forecast solar explosions of different intensities and in different forecast horizons. To do so, Multilayer Perceptrons with distinct configurations were adopted here and several experiments were made to assess the proper configuration of the MLPs and the best methodology to accomplish the desired goals.

In summary, the experimental results indicated that even though the errors increase with the extension of the forecast horizon, MLPs with a single output and specialized in predicting future values of a particular horizon led to the smallest mean-squared errors. Besides, it was also observed that to properly forecast solar explosions of different classes from the prediction of the X-ray flux series, it is mandatory that the training dataset is balanced. Otherwise, the resulting MLPs may introduce delays in the forecast, which is particularly dangerous in the context of this work.

In addition, it was observed that pure quantitative analysis of the results, such as the observation of average forecasting errors, may not be enough to assess the quality of the MLPs in the context of solar explosion forecast. In this work, the temporal delays observed in some of the experimental results were detected only through a careful visual inspection of the forecast series and comparisons with the original time series.

As future works, several extensions can be derived from this work. First, a larger time series of X-ray flux should be considered, particularly from different periods of the solar cycle, so the impact of distinct solar activity intensities can be evaluated. Second, different machine learning approaches could also be adopted instead of the MLPs, so that the best paradigm can be identified. Finally, wider forecast horizons could be explored.

Acknowledgments

The authors would like to acknowledge the financial support for this research through grant #2015/25568-5, São Paulo Research Foundation (FAPESP).

References

[1] R. Schwenn, "Space Weather: The Solar Perspective," *Living Reviews in Solar Physics*, vol. 3, no. 1, p. 2, 2006.

[2] G. D. Holman, "The Mysterious Origins of Solar Flares," *Scientific American*, vol. 294, no. 4, pp. 38–45, apr 2006.

[3] M. Youssef, "On the relation between the CMEs and the solar flares," *NRIAG Journal of Astronomy and Geophysics*, vol. 1, no. 2, pp. 172–178, dec 2012.

[4] D. Lenz, "Understanding and Predicting Space Weather," *Industrial Physicist*, vol. 9, no. 6, p. 18, 2004.

[5] M. C. Meirelles, "Um simples modelo SOC 2D para uma das maiores fontes de distúrbios geomagnéticos: Flares Solares," TCC, Universidade Federal Fluminense, 2012.

[6] M. G. Bobra and S. Ilonidis, "Predicting coronal mass ejections using machine learning methods," *The Astrophysical Journal*, vol. 821, no. 2, p. 127, apr 2016.

[7] S. W. P. Center, "NWS Space Weather Prediction Center," 2015. [Online]. Available: http://www.swpc.noaa.gov

[8] P. A. Morettin and C. M. C. Toloi, "Modelos para previsão de séries temporais," in *Colóquio Brasileiro de Matemática*. Poços de Caldas: IMPA, 1981.

[9] J. Han, M. Kamber, and J. Pei, *Data Mining: Concepts and Techniques*, 3rd ed. Illinois: Morgan Kaufmann Publishers, 2006.

[10] R. Qahwaji, T. Colak, M. Al-Omari, and S. Ipson, "Automated Prediction of CMEs Using Machine Learning of CME – Flare Associations," in *Solar Image Analysis and Visualization*. New York, NY: Springer New York, 2008, pp. 261–273.

[11] O. W. Ahmed, R. Qahwaji, T. Colak, P. A. Higgins, P. T. Gallagher, and D. S. Bloomfield, "Solar Flare Prediction Using Advanced Feature Extraction, Machine Learning, and Feature Selection," *Solar Physics*, vol. 283, no. 1, pp. 157–175, nov 2011.

[12] R. A. Calvo, H. A. Ceccato, and R. D. Piacentini, "Neural network prediction of solar activity," *Astrophysical Journal*, vol. 444, pp. 916–921, May 1995.

[13] A. Orfila, J. L. Ballester, R. Oliver, A. Alvarez, and J. Tintoré, "Forecasting the solar cycle with genetic algorithms," *Astronomy & Astrophysics*, vol. 386, no. 1, pp. 313–318, apr 2002.

[14] S. S. Haykin, *Neural networks and learning machines*, 3rd ed. Upper Saddle River, NJ: Pearson Education, 2009.

[15] J. Heaton, "Encog: Library of interchangeable machine learning models for Java and C#," *Journal of Machine Learning Research*, vol. 16, pp. 1243–1247, 2015.

[16] G. E. A. P. A. Batista, R. C. Prati, and M. C. Monard, "A study of the behavior of several methods for balancing machine learning training data," *SIGKDD Explor. Newsl.*, vol. 6, no. 1, pp. 20–29, Jun. 2004.